International Journal of Automotive Technology, Vol. 3, No. 4, pp. 129–135 (2002)

1229-9138/2002/004-01

COMPUTATIONAL DURABILITY PREDICTION OF BODY STRUCTURES IN PROTOTYPE VEHICLES

H. S. KIM[1)*], H. J. YIM[2)] and C. B. KIM[3)]

[1)]Hyundai Motor Company, 772-1 Changduk-Dong, Whasung-Si, Kyunggi-Do 445-706, Korea
[2)]Graduate School of Automotive Engineering, Kookmin University, Seoul 136-100, Korea
[3)]Division of Mechanical Engineering, Inha University, Incheon 402-751, Korea

(Received 12 March 2002; Revised 22 October 2002)

ABSTRACT–Durability estimation of a prototype vehicle has traditionally relied heavily on accelerated durability tests using predefined proving grounds or rig tests using a road simulator. By use of those tests, it is very difficult to predict durability failures in actual service environments. This motivated the development of an integrated CAE (Computer Aided Engineering) methodology for the durability estimation of a prototype vehicle in actual service environments. Since expensive computational costs such as computation time and hardware resources are required for a full vehicle simulation in those environments with a very long span of event time, the conventional CAE methodologies have little feasibility. An efficient computational methodology for durability estimations is applied with theoretical developments. The effectiveness of the proposed methodology is shown by the comparison of results of the typical actual service environment such as the city mode with those of the typical accelerated durability test over the Belgian road.

KEY WORDS : Computational durability estimation, Flexible multibody dynamic analysis, Dynamic stress analysis, Fatigue life prediction, City mode, Belgian mode, Degrees of freedom (DOFs)

1. INTRODUCTION

In developing process for a new vehicle, the appropriate criterion for durability design should be based on consideration of actual service environments of the vehicle. Experimental durability test may be the most exact method for durability evaluation of the prototype vehicle. But the test requires at least one prototype vehicle so that durability assessment should usually be performed with an accelerated rate in the later developing stage when the prototype vehicle are available. Therefore, it is impossible to achieve sign-off of durability estimation based on good consideration of actual service environments in the early developing stage. Early durability assessment is possible, however, if the necessary criterion is available through computer simulation. The current CAE (computer aided engineering) technology helps the designer to quantify the necessary information for durability design. Recent researches (Baek, Stephens and Dopker, 1993) (Kuo and Kelkar, 1995) (Yim and Lee, 1996) for integrated durability analysis have had computational shortcomings such as (1) high computational cost and hardware performance from very long event time and large scaled structural problems, (2) difficulties in computer simulation of actual service environments, (3) uncertainties of the fundamental database for durability analysis.

In this paper, an integrated computer aided durability analysis method with theoretical and technical improvements is proposed for efficient accurate durability estimation of a prototype vehicle with actual service environments. Necessity of the proposed methodology at the early developing stage is assured by a bus example. In the example, the method is demonstrated to show the comparison of the city mode, which is a typical actual service environment in the city, with the Belgian mode, which is a typical accelerated test environment on the Belgian road.

2. COMPUTER AIDED DURABILITY ANALYSIS

Computer aided durability analysis can be used in the design process by predicting possible problems in an early designs. Such analyses can substantially reduce industry's heavy reliance on extensive tests. Theoretical and technical developments, however, are necessary for durability estimation of a prototype vehicle under actual service environments.

*Corresponding author. e-mail: hskim001@hyundai-motor.com

This paper presents effective methodology, which consists of (1) flexible multibody dynamic analysis using deformation modes with reduced DOFs, (2) dynamic stress analysis using the hybrid superposition method, and (3) durability analysis integrated with previous two analyses and fatigue analysis.

3. THEORETICAL DEVELOPMENTS

3.1. Flexible Multibody Dynamic Analysis

Flexibility information in terms of deformation modes is obtained by finite element analysis of a structural component and used for flexible multibody dynamic analysis (Yoo and Haug, 1996). Deformation modes such as Ritz modes, Craig-Chang modes, or Craig-Bampton modes, etc. may be used.

In the case of using the finite element model of a large-scaled structural component that has large nodal degrees of freedom (DOFs), it becomes apparent that this large model is often inefficient. This motivates an efficient method, that is, flexible multibody dynamic analysis using reduced deformation modes (Kim and Kim, 2002), An original model with large nodal DOFs of the structural component is transformed to the reduced model with low nodal DOFs by use of reduction methods of nodal degrees of freedom. The reduced model has a static and dynamic characteristics correlated with that of the original one. By use of the component mode synthesis technique, the reduced deformation modes from the reduced model are obtained. The relation of the reduced and original deformation modes is expressed as

$$\boldsymbol{\psi}_R = \mathbf{T}\boldsymbol{\psi} \tag{1}$$

where $\boldsymbol{\psi}_R \subset R^{Nr}$ and $\boldsymbol{\psi} \subset R^{Nt}$ are the reduced and original deformation modes, respectively, and Nr and Nt (Nr < Nt) are DOFs. of the reduced and original model, respectively. $\mathbf{T} \subset R^{Nr \times Nt}$ is a transformation matrix to reduce DOFs.

3.2. Dynamic Stress Analysis

In order to improve the efficiency and accuracy of conventional methods (Baek, Stephens and Dopker, 1993) (Kuo and Kelkar, 1995) (Yim and Lee, 1996) (Ryu, Kim and Yim, 1996) for stress recovery, the hybrid superposition method (Kim, 1999) is developed. This method efficiently recovers the dynamic stress time histories by applying the principle of linear superposition to the mode acceleration method or static correction method. In this paper, the hybrid superposition method obtained from the mode acceleration method is briefly described.

Using stress recovery scheme of the method, dynamic stress $\boldsymbol{\sigma}(t)$ with the assumption of infinitesimal elastic deformation can be written as

$$\begin{aligned}\boldsymbol{\sigma}(t) = &\sum_{i=1}^{Ns} \mathbf{s}_{Si} p_{Si}^R(t) + \sum_{j=1}^{3} \mathbf{s}_{Gj} p_{Gj}^R(t) \\ &+ \sum_{k=1}^{6} (\mathbf{s}_{Ik} p_{Ik}^R(t) + \mathbf{s}_{Ck} p_{Ck}^R(t)) \\ &- \sum_{l=1}^{Nk} \left(\frac{2\xi_{Kl}}{\omega_{Kl}}\right) \mathbf{s}_{Kl} \dot{q}_{Kl}^R(t) \\ &- \sum_{m=1}^{Nk} \left(\frac{1}{\omega_{Km}^2}\right) \mathbf{s}_{Km} \ddot{q}_{Km}^R(t)\end{aligned} \tag{2}$$

where $a^R(t)$ $(a=p, q)$ means that a is time dependent function and calculated through flexible multibody dynamic analysis using reduced deformation modes in Equation (1). But on the other hand, stress coefficient vector $\mathbf{s}$ is time independent function and computed by finite element method. Ns and Nk are the number of components of surface loads and kept vibration modes, respectively. $p_{Si}^R(t)$, $p_{Gj}^R(t)$, $p_{Ik}^R(t)$ and $p_{Ck}^R(t)$ are time histories of i-th component of surface force, j-th component of gravity force, k-th component of D'Alembert inertia and Coriolis force, respectively. $\dot{q}_{Kl}^R(t)$ and $\ddot{q}_{Km}^R(t)$ are time histories of the velocity of l-th modal coordinates and acceleration of m-th modal coordinates, respectively. ξ_{Kl} and ω_{Kl} (l or m=1, ···, Nk) are the modal damping factor and the undamped circular natural frequency, respectively.

$\mathbf{s}_{Si}$ (i=1, ···, Nb), $\mathbf{s}_{Gj}$ (j=1, ···, 3), $\mathbf{s}_{Ik}$ and $\mathbf{s}_{Ck}$ (k=1, ···, 6) are static stress coefficients due to a unity of $p_{Si}^R(t)$, $p_{Gj}^R(t)$, $p_{Ik}^R(t)$ and $p_{Ck}^R(t)$ respectively, as follows;

$$\mathbf{s}_{ij} = \mathbf{D}\mathbf{B}\boldsymbol{\psi}_{Aij}, \quad i=S, G, I, C \tag{3}$$

where $\boldsymbol{\psi}_{Aij}$ is the j-th static correction mode with respect to the i-th group of forces. $\mathbf{D}$ is a matrix of elastic constants and $\mathbf{B}$ is a matrix that relates the vector of strain to the vector of nodal displacements. In the other hand, $\mathbf{s}_{Kl}$ and $\mathbf{s}_{Km}$ (l and m=1, ···, Nk) is modal stress coefficients due to a unit displacement of modal coordinates $q_{Kl}^R(t)$ or $q_{Km}^R(t)$, as follows;

$$\mathbf{s}_{Kl} = \mathbf{D}\mathbf{B}\boldsymbol{\phi}_{Ki} \tag{4}$$

where $\boldsymbol{\phi}_{Ki}$ is the i-th vibration normal mode.

In Equation (2), the first 4 terms in the right hand side are pseudostatic stresses, which may affect force induced stresses or fatigue damages. The remaining terms are modal velocity stresses and modal acceleration stresses, which may affect vibration induced stresses or fatigue damages.

The proposed stress analysis method is executed in three steps. In the 1st step, time dependent functions such as time histories of dynamic loads, modal coordinates and gross body motion, etc are calculated efficiently through flexible multibody dynamic analysis using reduced deformation modes in Equation (1) from the reduced model. In the 2nd step, time independent functions such as stress coefficients in Equation (3) and Equation (4) are obtained precisely through finite element analyses using original model. In the final step, dynamic stress time

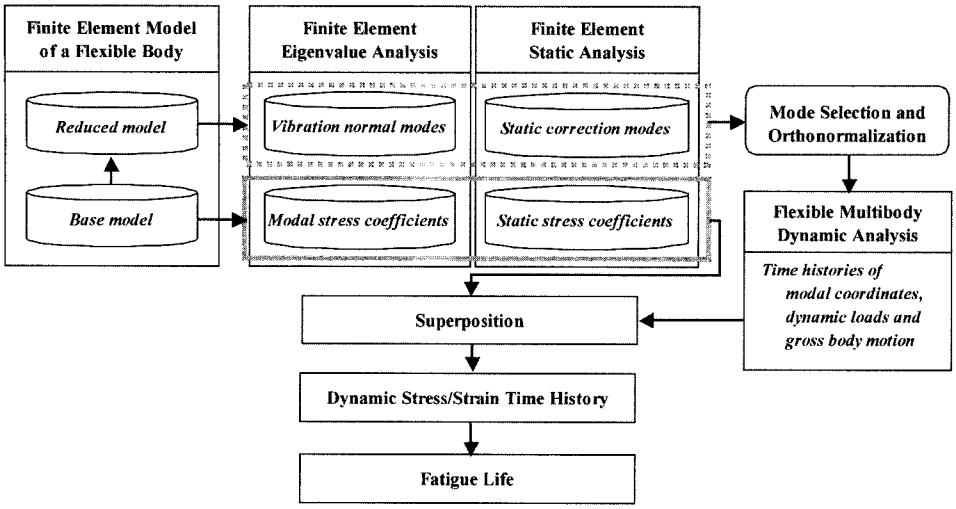

Figure 1. Conceptual procedure and data flow.

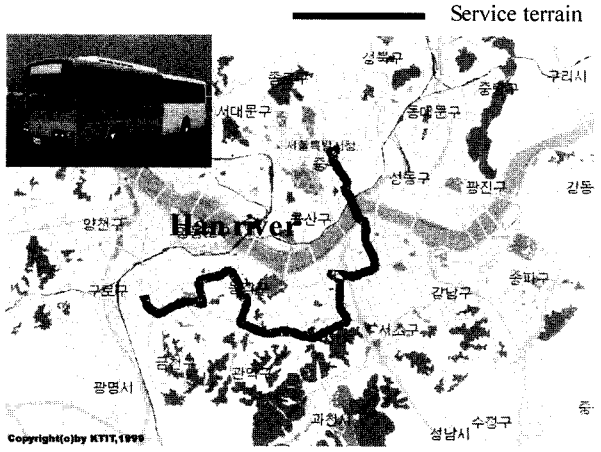

Figure 2. Typical service terrain of a city bus in the Seoul Metropolis.

histories are recovered through hybrid superposition according to Equation (2).

3.3. Integrated Durability Analysis

The integrated durability analysis can be implemented as Figure 1, which shows an outline of the proposed methodology and its conceptual data flow.

4. DURABILITY ESTIMATION

4.1. Scenario

The simulation scenario is the city mode for which the driving course is shown in Figure 2. The course is typical service terrain of a city bus in the Seoul metropolis, of which total distance is about 22.5 km. The Belgian mode

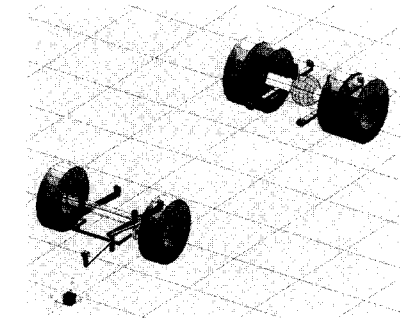

(a) Multibody model of the bus

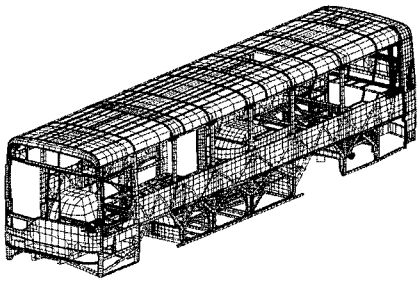

(b) Finite element model of the body structure

Figure 3. Multibody model.

is adopted for a comparative study. The Belgian block in the proving ground is 0.8 km. The prototype city bus to be investigated is shown in Figure 2.

4.2. Flexible Multibody Dynamic Analysis

For multibody dynamic analysis to obtain time dependent terms in Equation (2), a general purpose multibody dynamic analysis code (DADS, 1995) is used. The

multibody dynamic model of the bus is composed of a chassis and a body structure as shown in Figure 3.

The chassis, which consists of a rigid axle type suspension system and an axle driving system, is composed of 128 rigid bodies that are constrained by kinematic joints and constraints. The axle driving system consists of 4 axle spindle drivers. To include nonlinear effects of components in the suspension system, nonlinear properties measured from experiments are used.

In general, road profiles and tire models are necessary for the vehicle driving simulation. Road profiles must be obtained from actual measurements on service roads. Durability oriented tire modeling is also difficult. These two indispensable difficulties may increase costs and inaccuracy of the simulation. Therefore axle-driving technique is proposed for driving simulation. This technique is the simulation method reproducing driving environment by employing axle spindle displacement time histories as driving constraint conditions. The axle spindle displacement time histories are gained from signal processes including twice time integration and band-pass filtering of axle spindle acceleration signals. The axle spindle acceleration signals are measured from actual drives of the prototype bus with a half GVW (Global Vehicle Weight) in the city mode shown in Figure 2 with maximum 65 km/h and the Belgian mode with a constant velocity, 25 km/h. As typical behaviors, the vertical displacement time histories at the left-hand side axle spindle of the front axle are shown in Figure 4. In the city mode, severe movements are rised around 930.0 sec by passing on rough road under subway construction. The movement in the Belgian mode, however, is severer than in city mode. RMS (Root Mean Square) values of histories in city and the Belgian mode are 1.9085E-3 and 9.9426E-3, respectively. The RMS value of the Belgian mode is 5.2094 times larger than the one of the city mode.

In the other hand, the body structure is modeled as a flexible body in order to consider flexibility effect. As shown in Figure 3. (b), the body structure of the bus is composed of 5 sub parts, that is, a roof, a front body, a rear body, a center body and a frame. The frame is fabricated to the suspension system using 18 joints. Through those joints, suspension loads are transmitted to the body structure. Mechanical parts, such as engine, air conditioner, and other nonstructural masses are attached to corresponding nodes of the body structure with spring and damper elements. The finite element model of the body structure, which consists of 47,152 nodes and 46,744 elements and has 282,912 DOFs. This original model has very large DOFs so that the dynamic analysis and its pre-processing are very difficult. To improve efficiency, reduced deformation modes are utilized as described in the previous section. The reduced model with total 1236 master DOFs as shown in Figure 5. (a) is obtained from the original one. Reduced deformation modes are selected as Craig-Chang modes obtained from the reduced model. Those modes are ortho-normalized modes of 20 vibration modes in frequency range to 50 Hz and 8 inertia relief attachment modes that are obtained by imposing unity vertical forces on each mounting joint between the body structure and leaf springs. The fundamental torsion mode among deformation modes is shown in Figure 5. (b) MAC (Modal Assurance Criteria) value of each corresponding mode is above 0.95. Through this DOF reduction, the flexible multibody dynamic analysis will be efficiently performed.

In dynamic analysis, the initial conditions of the bodies must be defined at the start of the analysis. it is necessary to specify initial conditions for only the independent

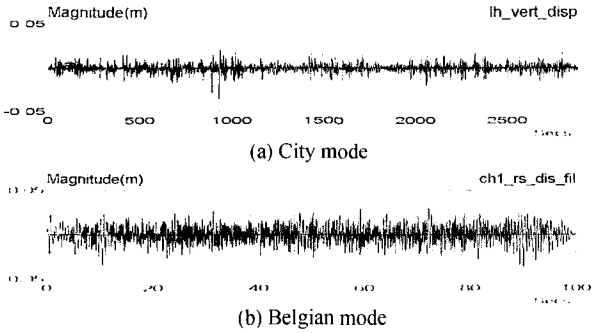

(a) City mode

(b) Belgian mode

Figure 4. Typical vertical displacement of the front left-handside axle spindle.

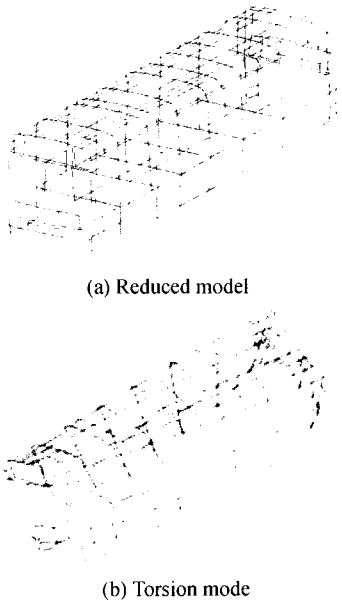

(a) Reduced model

(b) Torsion mode

Figure 5. Reduced model and its vibration mode.

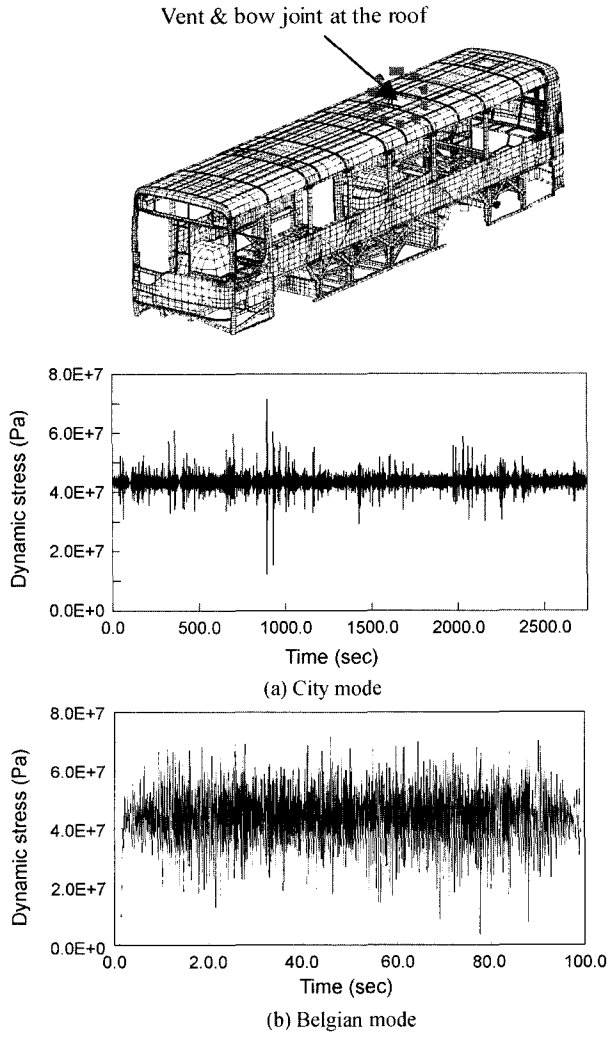

Figure 6. Comparison of typical dynamic stress time history.

coordinates, of which the number is equal to the number of DOFs, that is, total independent 148 DOFs with 28 flexibility DOFs. Equilibrium analysis at initial simulation time was performed to identify these independent coordinates. Initial values of the identified independent coordinates were used for the complete dynamic simulation. In the city mode, total event time is from 0.0 sec to 2900.0 sec, the maximum integration step-size is 0.001 sec and the print step-size is 0.005. Total steps fed into the next step, then, are 580,001 steps. In the other hand, In the Belgian mode, total event time is from 0.0 sec to 95.0 sec and the other conditions are the same as the city mode. Total steps, then, are 19,001 steps. From the simulation, various dynamic results such as time histories of dynamic loads, modal coordinates and gross body motion of the body structure are obtained.

4.3. Dynamic Stress Analysis

For stress analysis to obtain time independent terms such as stress coefficients, a general purpose finite element analysis code (MSC/NASTRAN, 1997) is used. The critical element sorting technique that can identify a small number of highly sensitive 100 elements for each stress coefficients in Equation (2) is developed. Static stress coefficients and modal stress coefficients for 1,236 critical elements are calculated through static and eigenvalue analyses by use of the original model, that is, a stress oriented finite element model. Time histories of various dynamic results are accurately predicted in the previous step. Finally, Dynamic stress time histories are obtained from stress superposition according to Equation (2). Figure 6. (a) and (b) show the dynamic stress at the critical element in the joint of the roof center vent and bow, which are obtained in the city and Belgian mode, respectively. These figures show that mean stresses are similar but distribution of stress peaks is different each other.

4.4. Fatigue Life Prediction

In this paper, the local strain life method using an established fatigue life prediction code (P3/FATIGUE, 1997) is employed to predict fatigue life of critical elements in the body structure. Fatigue analyses are performed to predict crack initiation lives of critical elements by use of fatigue properties of the SAE1020-HR material. Table 1 gives the lowest 5 fatigue lives from results of the durability analysis of the city and Belgian modes. In the table, (1) the order of crack initiation in Num. 1~Num. 4 except the Num. 5 are the same each other, and (2) the severity of the Num. 5 is relatively small compared to the other. These are originated from the difference of stress characteristics in two durability modes as shown in the previous section.

In order to understand the relation between stress characteristics and fatigue damage, frequency correlated normalized damages are shown in Figure 7. Figure 7. (a) shows that the reason for the different order and relatively small severity in the Num. 5. In the city mode, fatigue damage in wide banded frequency range above 25 Hz makes a relatively large contribution to total fatigue life due to the vibration induced fatigue damage. This fatigue damage is caused from the modal acceleration stresses by the roof structures bending vibration. But, in the Belgian mode, fatigue damage in narrow banded frequency range below 15 Hz makes a main contribution to total fatigue life due to the force induced fatigue damage. This fatigue damage is caused from the pseudostatic stresses by dynamic loads applied from the suspension system. In the other hand, Figure 7. (b) shows that a reason for the similar severity in the Num. 1~4, in which the distribution of fatigue damage in the city mode have a similar

Table 1. Comparison of durability modes.

Num	Critical area	Error[1] (%)	Fatigue life[2]		Severity[3]
			City	Belgian	
1	RH[4] rear cant rail joint	19	1	1	38.0
2	Middle door's rear pillar joint	27	2	2	47.7
3	LH[5] rear cant rail joint	17	3	3	44.6
4	RH rear side frame	29	5	4	69.0
5	Roof vent's joint	23	4	16	12.5

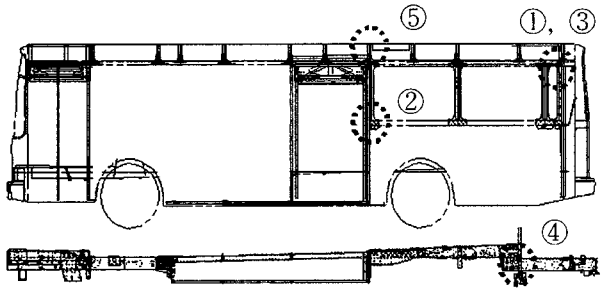

(1) The error of fatigue life in the Belgian mode:
Diff (%)=| (Analysis–Test) ÷ Test | × 100(%)
(2) The order of crack initiation
(3) Severity = life in the city ÷ life in the Belgian
(4) RH: Right-Hand side
(5) LH: Left-Hand side

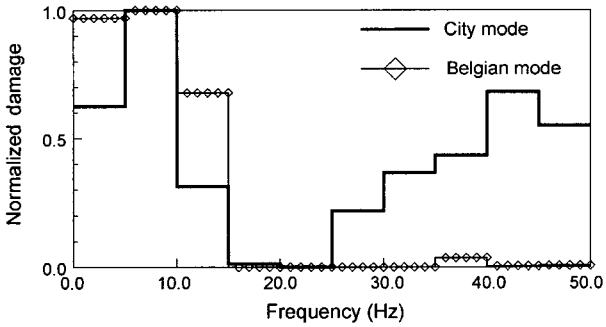

(a) Roof vent's joint (⑤)

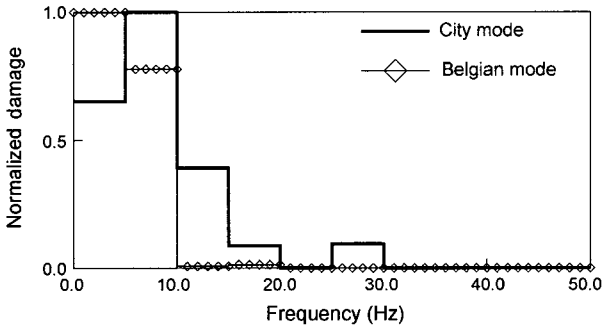

(b) LH rear cant rail joint (③)

Figure 7. Frequency correlated normalized damage.

trend to that in the Belgian mode.

As an example of the correlation in the Belgian mode, Figure 8 shows that the position of crack initiation in the most sensitive area in analysis is the same as that of the test. The position of the joint, that is, the LH rear cant rail joint is referenced in the Table 1. The average of crack

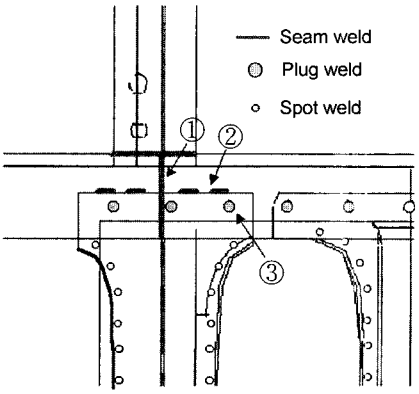

(a) Geometry

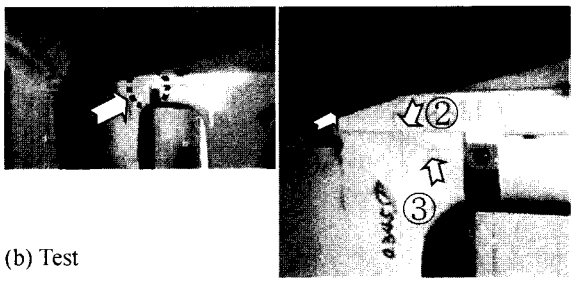

(b) Test

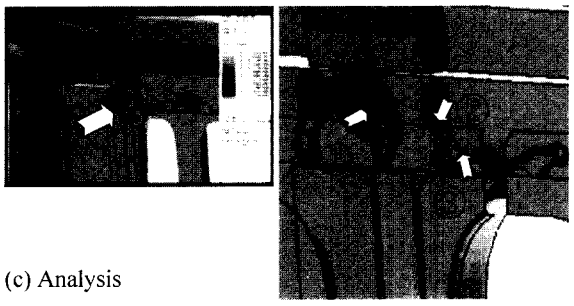

(c) Analysis

Figure 8. Comparison of the test and analysis in the Belgian mode.

initiation time of the three areas (①, ②, ③) in Fig. 8 has the difference of 17% from results of the test and analysis in the Belgian mode, respectively. This represents a successful correlation.

5. CONCLUSIONS

This research presents an efficient methodology for the integrated durability analysis that consists of flexible multibody dynamic analysis, dynamic stress one, and fatigue one with theoretical and technical developments. The durability of the body structure in the investigated prototype bus has the following characteristics. In the Belgian mode, the total fatigue damage is mainly affected by the force induced fatigue damage below 15 Hz, which is caused from the pseudostatic stresses by dynamic loads applied from the suspension system. In the other hand, in the city mode, the total fatigue damage of flexible subparts such as roof structure can be largely affected by the structural vibration induced fatigue damage in higher frequency range above 15 Hz, which is caused from the modal velocity and acceleration stresses.

The durability of a prototype vehicle has been traditionally estimated in accelerated test environments such as the Belgian mode. However, durability of critical areas where a vibration induced fatigue damage make a large contribution to total one, must be assured in actual service environments such as the city mode, instead of accelerated test environments. Durability test in actual service environments such as the city mode, however, should require very long periods above a few years. Therefore the proposed computational methodology can be used as an efficient and reliable means for the sign-off of durability of a prototype vehicle with actual service environments in the early-developing stage.

REFERENCES

Baek, W. K., Stephens, R. I. and Dopker, B. (1993). Integrated computational durability analysis, *ASME J. of Eng. for Industry*, **115**.

DADS User's Manual Rev. 8.0. (1995). Computer Aided Design Software, Inc., IA 5221.

Kim, H. S. (1999). *Dynamic Stress Analysis of a Flexible Body in Multibody System for Fatigue Life Prediction.* Ph.D. Thesis, The Univ. of Inha, Korea

Kim, H. S. and Kim, C. B. (2002). Flexible multibody dynamic analysis using reduced deformation modes, *Proc. of the First Asian Conference on Multibody Dynamics,* No. T313, 201–208.

Kuo, E. Y. and Kelkar, S. G. (1995). Vehicle body structure durability analysis. *SAE Paper No.* 951096.

MSC/NASTRAN User's Manual Ver. 70. (1997). The MacNeal-Schwendler Corporation.

P3/FATIGUE User's Manual Ver. 70. (1997). The MacNeal-Schwendler Corporation.

Ryu, J., Kim, H. S. and Yim, H. J. (1996). An efficient and accurate dynamic stress computation by flexible multibody dynamic system simulation and reanalysis, *KSME Int. J.* **11**, **4**, 386–396.

Yim, H. J. and Lee, S. B. (1996). An integrated CAE system for dynamic stress and fatigue life prediction of mechanical systems, *KSME Journal*, **10**, **2**, 158–168.

Yoo, W. S. and Haug, E. J. (1996). Dynamics of articulated structures, Part I.: Theory. *J. of Struc. Mech.*, **14**, **1**, 105–126.

APPENDICES

A.1 Frequency correlated normalized damage

Fatigue damage distribution in the frequency domain can be identified by use of the frequency correlated normalized damage. This method gives a relative contribution of fatigue damage for each frequency band to total one. This is computed as follows;

Step 1. If the stress-life method or the strain-life method are used, the damage can be calculated by time histories of stress $\sigma(t)$ or strain $\varepsilon(t)$, respectively.
Set $\xi = \sigma$ or ε
where σ or ε mean the stress or strain life method, respectively.

Step 2. Compute total damage D^{ξ} by use of $\xi(t)$.

Step 3. Set i=1

Step 4. Devide total frequency range into finite frequency bands by an increment Δf. The total number of frequency band is Nb. The i-th frequency band Δf_i is from f_i^S to f_i^E.
$\Delta f_i \in (f_i^S, f_i^E)$
where $f_i^S = f_1^S + (i-1)\Delta f$
$f_i^E = f_i^S + \Delta f$

Step 5. Filter out frequency components corresponding to the Δf_i from $\xi(t)$ by use of a low and high pass filter of the frequency range Δf_i. And get the filtered time histories $\tilde{\xi}_i(t)$.

Step 6. Compute the damage D_i^{ξ} from $\tilde{\xi}_i(t)$.

Step 7. Gain the frequency correlated damage D_i^{ξ} of Δf_i.
$D_i^{\xi} = D^{\xi} - D_i^{\xi}$

Step 8. If i=Nb, then goto step 9,
else set i=i+1and goto step 4.

Step 9. Normalize D_i^{ξ} with respect to the maximum damage $\mathrm{Max}D^{\xi}$. And get the frequency correlated normalized damage d_i^{ξ}.

$$d_i^{\xi} = \frac{D_i^{\xi}}{\mathrm{Max}D^{\xi}}, \quad i=1, \mathrm{Nb}$$

where $\mathrm{Max}D^{\xi} = \max(D_i^{\xi}, i=1, \mathrm{Nb})$